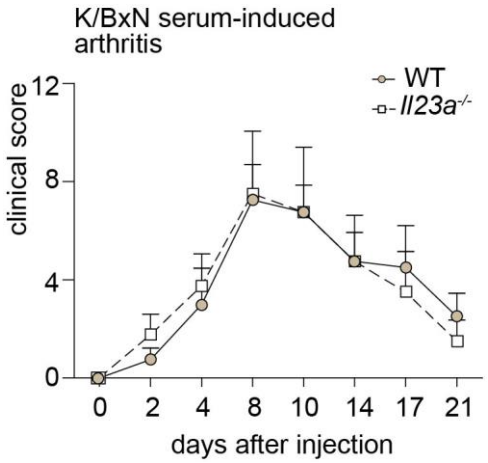

Supplementary Figure 1

Il23a$^{-/-}$ mice develop regular arthritis induced by the transfer of K/BxN serum.

(**a**) Clinical scoring of arthritis in wild type (WT) and *Il23a*$^{-/-}$ mice that received serum from arthritic K/BxN mice. Error bars represent SEM *P<0.05; **P<0.01; ***P<0.001; Student's t test.

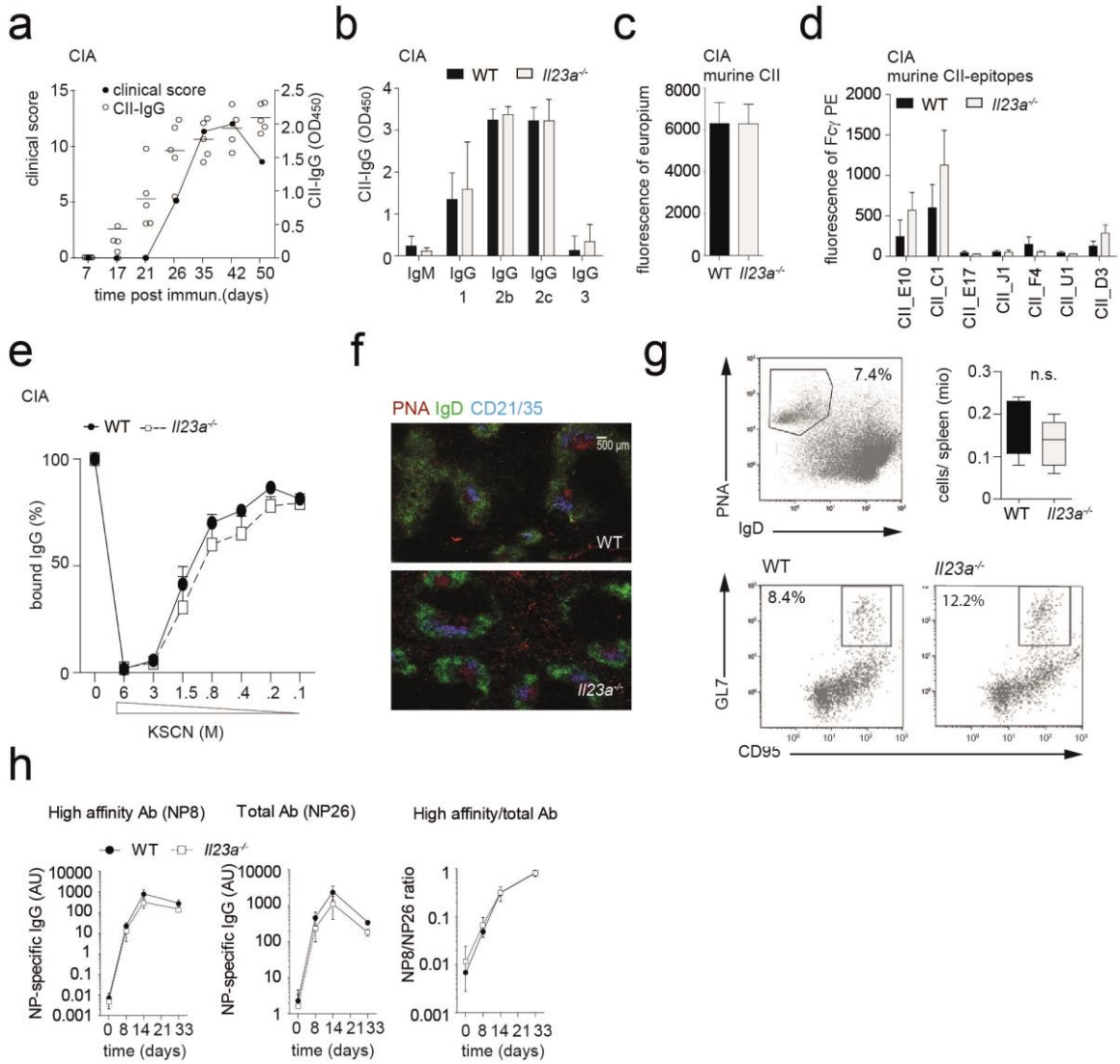

Supplementary Figure 2

Humoral immune response in wild-type and *Il23a*$^{-/-}$ mice during CIA.

(**a-d**) Analysis of levels of (**a**) collagen type II (CII)-specific IgG, (**b**) CII-specific IgG subsets, (**c**) IgG specifically directed against murine CII (**d**) and IgG detecting different murine CII epitopes in the sera of WT and *Il23a*$^{-/-}$ mice at day 50 after induction of collagen-induced arthritis (CIA). (**e**) KSCN titration assay for the determination of the binding affinity of CII-specific IgG in WT and *Il23a*$^{-/-}$ mice. (**f,g**) Analysis of the appearance of (**f**) germinal centers and the appearance of germinal center (CD19 pre-gated) B cells (**g**) at day 26 after induction of CIA in WT and *Il23a*$^{-/-}$ mice. (**h**) Measurement of the levels of regular and high affinity antibodies in response to a T cell dependent immunization with 4-hydroxy-3-nitrophenylacetyl (NP) coupled to chicken g-globulin (NP-CGG) in WT and *Il23a*$^{-/-}$ mice. Error bars represent SEM*P<0.05; **P<0.01; ***P<0.001; Student's t test.

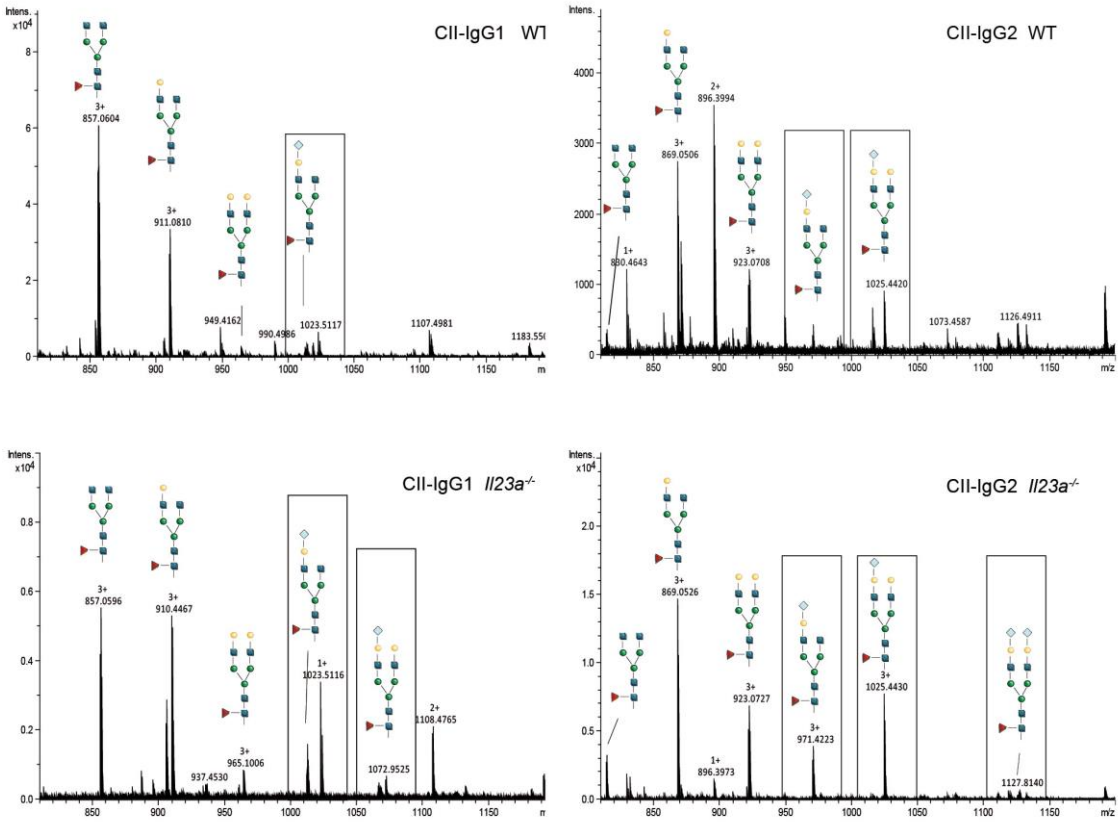

Supplementary Figure 3

Analysis of the glycostructure of CII-specific IgG by mass spectrometry.

Representative mass spectra illustrating IL-23-dependent changes of the glycosylation at Asn-297 of the indicated IgG subclasses of collagen type II-specific IgG isolated from the sera of WT and *Il23a*$^{-/-}$ mice at day 50 after induction of CIA.

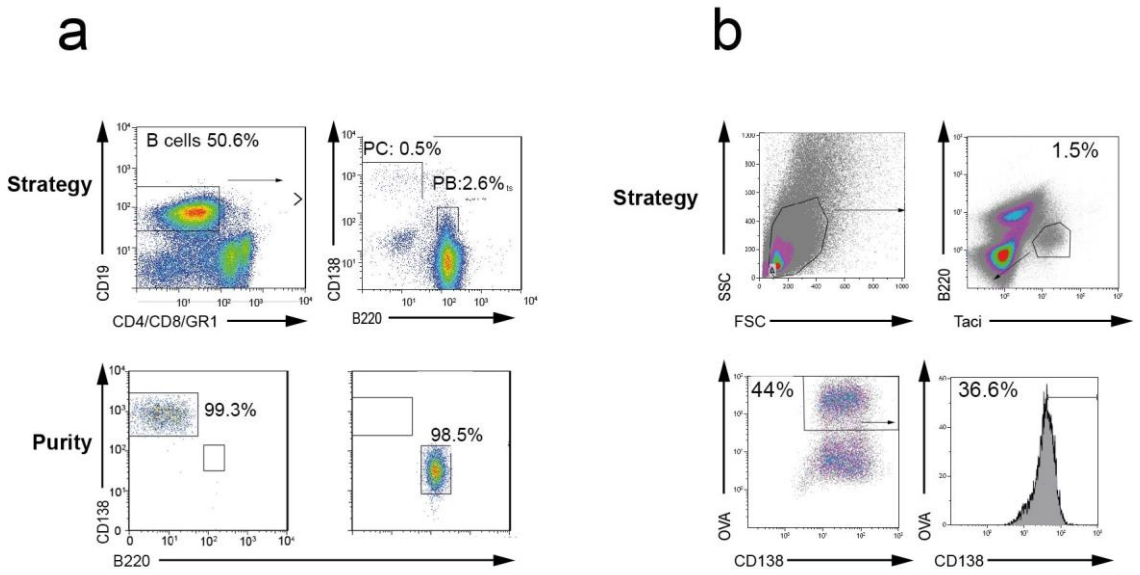

Supplementary Figure 4

Identification of plasma cells and plasmablasts.

(**a**) Sorting strategy and sorting purity analysis of splenic plasma cells ($CD19^{+}CD138^{+}B220^{-}$) and plasmablasts ($CD19^{+}CD138^{low}B220^{+}$) for mRNA-analysis. (**b**) Gating strategy for the flow cytometric analysis of St6gal1 protein expression in splenic Ova-specific plasmacells and plasmacells isolated during collagen-induced arthritis. Plasmacells were gated to be $B220^{low}CD138^{+}Taci^{+}$ and Ova^{+}, respectively.

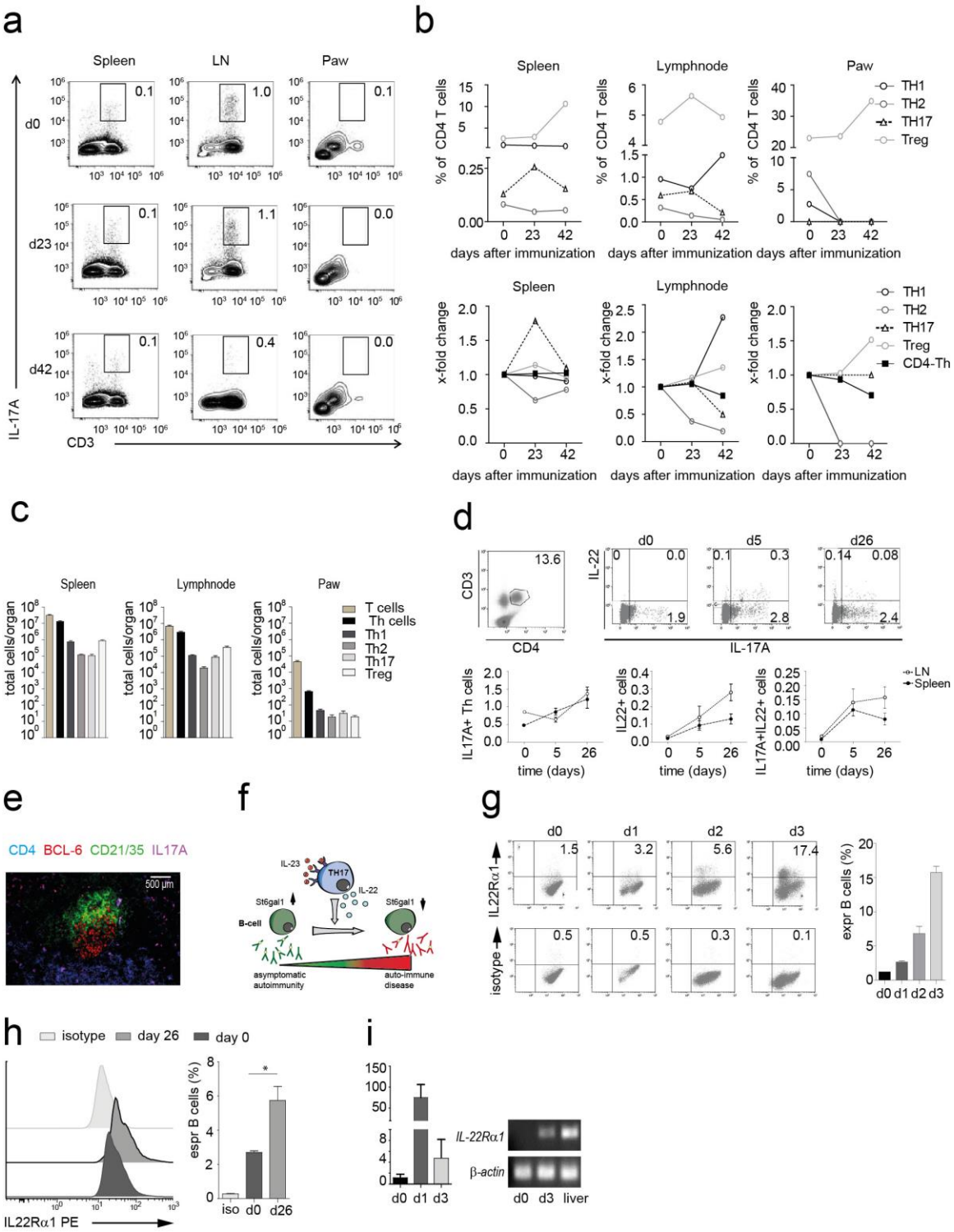

Supplementary Figure 5

Characterization of the T_H17 response during CIA.

(**a**) Flow-cytometric analysis of the content of IL-17-expressing $CD3^+$ T cells in spleen, inguinal lymph nodes (LN) and paws of wild-type (WT) DBA mice at indicated time points during the course of collagen-induced arthritis (CIA). (**b**) Mean percentage and fold change of the numbers as well as (**c**) total cells/organ of indicated T cell subsets in spleen, LN and

paws of WT DBA/1 mice at indicated time points after induction of CIA. $CD4^+CD3^+$ T cells were subcategorized into IFNγ-expressing Th1 cells, IL-4-expressing Th2 cells, IL-17-expressing T_H17 cells and FoxP3-expressing Treg cells. (**d**) Frequency of IL-17-positive, IL-22-positive and IL-17/IL-22 double-positive T cells in spleens and lymph nodes of WT mice at the indicated time points after induction of CIA. (**e**) Identification of $CD4^+$Bcl-6^+IL17^+ T cells within germinal centers of the spleen 26 days after induction of CIA (**f**) Proposed model of the IL23/Th17-mediated control of autoantibody activity. (**g**) Flow cytometry-based quantification of the expression of the IL-22 receptor (IL22Rα1) on $CD19^+B220^+$ B cells that were differentiated into plasmablasts by incubation with LPS (5μg/ml). (**h**) Quantification of IL-22 receptor (IL-22Rα1) surface expression on splenic $CD19^+B220^+$ B cells at day 0 and day 26 after induction of CIA. (**i**) mRNA expression of IL22Ra1 in in vitro differentiating plasmacells. Error bars represent SEM*P < 0.05, **P < 0.01, ***P < 0.001; Student's t test. Error bars represent SEM*P < 0.05, **P < 0.01, ***P < 0.001; Student's t test.

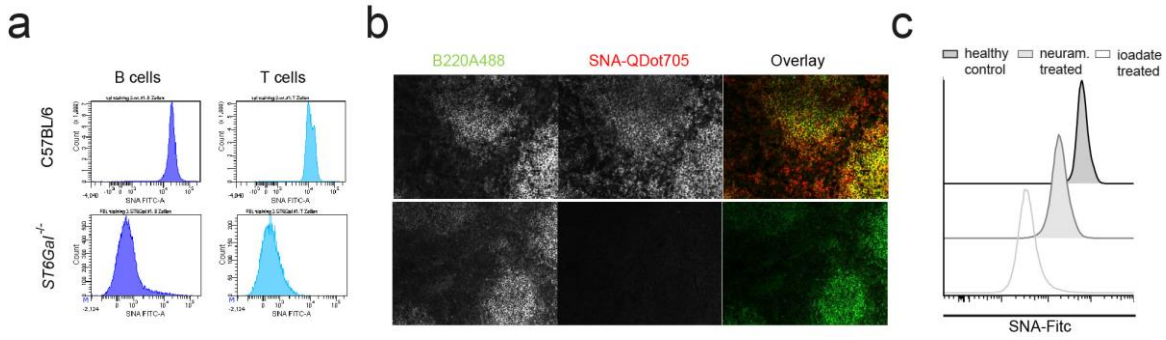

Supplementary Figure 6

Evaluation of the specificity of SNA lectin surface staining for determination of cellular St6gal1 activity.

(**a**) B and T cells of wild-type (WT) and *St6gal1*$^{-/-}$ mice were stained with a FITC-coupled SNA-lectin to determine the levels of surface sialic acid. (**b**) Immunofluorescence microscopy of spleens of WT and *St6gal1*$^{-/-}$ mice determining the levels of sialic acid on B220^{+} B cells by co-staining with an antibody against B220 (A488, green) and a SNA lectin (QDot705, red). (**c**) Human CD19^{+} B cells were stained with FITC-stained SNA-lectin to determine the levels of surface sialic acid. B cells were pre-treated with neuraminidase (100 mU , 1h at 37°C) or iodate (2mM, 1h at 4°C) to remove sialic acid where indicated. Error bars represent SEM*P < 0.05, **P < 0.01, ***P < 0.001; Student's t test.